Desalination and Water Treatment
www.deswater.com
doi: 10.1080/19443994.2014.937751

55 (2015) 1973–1980
August

Taylor & Francis
Taylor & Francis Group

Hybrid Fe_3O_4/MOFs for the adsorption of methylene blue and methyl violet from aqueous solution

Ling Li*, Li Jun Yuan, Wei Hong, Lu Fan, Le Bao Mao, Li Liu

Hubei Collaborative Innovation Center for Advanced Organic Chemical Materials, Hubei University, 430062 Wuhan, P.R. China, Tel. +68 27 88662747; Fax: +68 27 88663043; emails: waitingll@yahoo.com (L. Li), 765770283@qq.com (L.J. Yuan), 2212606889@qq.com (W. Hong), 824108937@qq.com (L. Fan), 1040877716@qq.com (L.B. Mao), 654225964@qq.com (L. Liu)

Received 23 September 2013; Accepted 20 May 2014

ABSTRACT

The adsorptions of methylene blue (MB) and methyl violet (MV) from an aqueous solution of Fe_3O_4/metal-organic frameworks (MOFs) composite were studied in view of the adsorption isotherm, kinetics and regenerate of the sorbent. The adsorption isotherms of MB and MV on Fe_3O_4/MOFs composite both followed the Langmuir isotherm. Adsorption kinetics were determined from the experimental data. The used Fe_3O_4/MOFs could be regenerated by acetonitrile, so it can be recycled for use. The excellent adsorption effect and reusability make Fe_3O_4/MOFs attractive for the removal of MB and MV from aqueous solution. The feasibility of Fe_3O_4/MOFs for application in magnetic solid-phase extraction was examined.

Keywords: Fe_3O_4/MOFs; Methylene blue; Methyl violet; Adsorption; Determination

1. Introduction

In daily life, more than 100,000 types of commercial dyes are used with a production of over 7×10^5 tons annually [1,2]. Many are considered to be toxic and even carcinogenic, and most toxic dyestuffs are stable to light and oxidants, which makes them difficult to degrade [3].

There are many technologies used for the removal of dyestuffs, and adsorption technology is regarded as one of the most competitive methods because of its wide application scope, excellent treatment effect, and recovery of valuable products and raw materials [4,5]. Methylene blue (MB) and methyl violet (MV) are most common stains. MB and MV contaminants not only deteriorate water quality, but also make a significant impact on human health due to toxic, carcinogenic, mutagenic or tetratogenic effects. So it is still a great significance to discover new materials for efficient removal of MB and MV.

In the past decades, metal-organic frameworks (MOFs) have drawn a growing interest among the scientific community owing to their high porosity and tenability [6–8]. MOFs have a broad potential application in chiral catalysis, adsorption, separation, and gas storage. All these receive a considerable amount of attention, but there are only a few articles about aqueous solution adsorption onto MOFs, and the research about application of MOFs in wastewater treatment is relatively rare. However, it is found that MIL-101 (MOFs of Cr) is with greater adsorption capacity for dyes compared to activated carbon, which can be used in high concentration dyeing wastewater treatment [9]. In addition, MIL-101 can be reused after being washed with lye. Therefore, MOFs are expected to be used as adsorbent in the application of dyeing wastewater

*Corresponding author.

treatment. The choice of MOFs as adsorbents is fostered by the large surface areas of these materials [10–13].

Nevertheless, MOFs exhibit a few weak points that impact their potential use. These include the poor stability in humid conditions as well as weak dispersive forces [14]. Furthermore, the open framework of MOFs is not able to provide strong, non-specific adsorption forces, so it is difficult to retain small molecules at ambient conditions. Combining MOFs with other substrates has been proposed in order to mitigate the above-mentioned drawbacks [15].

Magnetic hybrid materials based on magnetic inorganic material and non-magnetic adsorbent material take advantage of the combined benefits of both materials, which exhibit excellent adsorption efficiency and rapid separation from the matrix by an external magnetic field, and have recently exhibited significant advantages in separation science. Magnetic separation based on the super paramagnetic Fe_3O_4 is obviously much more convenient, economic and efficient, and the composite of Fe_3O_4 is widely used in sample pretreatment procedures [16,17].

Based on the above considerations, Fe_3O_4/MOFs composite is prepared. The adsorptions of MB and MV on Fe_3O_4/MOFs are studied in respect of adsorption isotherm, and kinetics. The possibility of using Fe_3O_4/MOFs as adsorbents for the removal of dyes from wastewater is discussed. The feasibility of Fe_3O_4/MOFs for the application in magnetic solid-phase extraction (MSPE) is examined, and the method of determination of trace amount of MB and MV is tested.

2. Experimental

2.1. Reagents and materials

All chemicals were at least of analytical grade. $FeCl_3{\cdot}6H_2O$, $FeSO_4{\cdot}7H_2O$, and $NH_3{\cdot}H_2O$ were used to prepare Fe_3O_4 nanorods. $Cu(Ac)_2{\cdot}H_2O$, dimethylfomamide (DMF) and terephthalic acid (H_2BDC) (Aladdin, Shanghai, China) were used to prepare Fe_3O_4/MOFs. Ultrapure water (18.2 MU cm) was obtained from a WaterPro Water Purification System (Labconco Corporation, Kansas City, MO, USA). Aqueous stock solutions of MB (18.70 mg L^{-1}) and MV (20.40 mg L^{-1}) were prepared by dissolving MB and MV in ultrapure water. The MB concentrations were determined using ultraviolet spectrophotometer at 665 nm, and the MV concentrations were determined using ultraviolet spectrophotometer at 577 nm, respectively. The calibration curve was obtained from the spectra of standard solutions, which was used to determine the residual concentration of MB or MV in solution.

2.2. Synthesis of Fe_3O_4 and Fe_3O_4/MOFs

The Synthesis of Fe_3O_4 and Fe_3O_4/MOFs was based on reference [18], and the detailed information was as followed:

2.7 g (10 mmol) $FeCl_3{\cdot}6H_2O$ and 2.7 g (10 mmol) $FeSO_4{\cdot}7H_2O$ were dissolved in 60 mL ultrapure water; transferred to a 250 mL flask in 30˚C water bath and magnetic stirring, then 25% $NH_3{\cdot}H_2O$ was added to form precipitation till pH ≥ 10, up to 80˚C; the reaction was kept for 30 min; the obtained Fe_3O_4 nanorods were washed with ultrapure water and ethanol three times, and then dispersed in ethanol, dried, and stored for use.

0.395 g (2.38 mmol) terephthalic acid was dissolved in 40 mL DMF and 40 mL ethanol was added; 0.07 g Fe_3O_4 nanorods was added in magnetic stirring, heated, and refluxed for back half an hour in 70. The solution of 0.86 g (4.31 mmol) $Cu(Ac)_2{\cdot}H_2O$ dissolved in 40 mL ultrapure water was added to keep reaction for 4 h; then the solid was obtained through centrifugation, washed by ultrapure water (50 mL) and ethanol (10 mL × 3), dried for 10 h in 120˚C; and Fe_3O_4/MOFs was obtained.

2.3. Characterization of the Fe_3O_4/MOFs

The crystalline structure of Fe_3O_4/MOFs was identified by a D/max-IIIC X-ray diffractometer (Shimadzu, Japan). Fourier transform infrared (FT-IR) spectra were taken with a Spectrum One FT-IR spectrophotometer (Perkin-Elmer, America) at room temperature. Scanning electron microscope (SEM) (Model EPMA-8705QH2, Shimadzu Co., Japan) was used to observe the morphologies of Fe_3O_4/MOFs. N_2 adsorption–desorption analysis was performed on an Accelerated Surface Area and Porosimetry System ASAP2020 (Micromeritics, American).

2.4. Adsorption experiments

The adsorbent Fe_3O_4/MOFs (10.0 mg) were added to the aqueous solution of MB (5 mL) with 3.74 mg L^{-1}. The mixture was well oscillated for a fixed time (5–60 min) at 298 K. After adsorption, the solution was magnetically separated, and the concentration of residual MB was determined by UV–vis spectrophotometer at 665 nm. For a kinetic study, the supernatant was collected at different time intervals for the determination of unabsorbed MB.

The study on the adsorption of MV was the same way to MB. Residual MV was determined at 577 nm.

2.5. Desorption experiments

The feasibility for regenerating the exhausted Fe_3O_4/MOFs was evaluated using the solvent desorption technique. Solutions of methanol, ethanol, acetone and glycol were tested as the eluent to regenerate Fe_3O_4/MOFs. The eluent solution was added to the used Fe_3O_4/MOFs and the mixture was ultrasonicated for half an hour.

2.6. Magnetic solid-phase extraction procedures

The entire extraction procedure using Fe_3O_4/MOFs as absorbent is shown as following: First, 5 mg sorbent was dispersed into a 5 mL aqueous sample solution, the mixture was shaken for 30 min to reach adsorption equilibrium, and then a strong magnet was deposited at the bottom of the beaker to isolate the sorbent from the sample solution. After approximately 1 min, the suspension became limpid and the liquid was decanted. After washing with 5 mL of methanol, the preconcentrated target analytes were eluted from the sorbent with 2 mL of acetonitrile after ultrasonicating for 30 min. One milliliter of the elute was diluted to 10 mL for analysis by ultraviolet spectrophotometer.

3. Results and discussion

3.1. Characterization results

Powder XRD patterns of Fe_3O_4 and Fe_3O_4/MOFs are shown in Fig. 1(a). The diffraction peaks of Fe_3O_4 match well with relative reference [18], which shows Fe_3O_4 are well crystallized. The diffraction peaks of Fe_3O_4 are weak in Fe_3O_4/MOFs, because the content of Fe_3O_4 is very little in composite, and crystal peaks of MOFs appear in Fe_3O_4/MOFs [19] indicating the formation of composite Fe_3O_4/MOFs.

Further confirmation of Fe_3O_4/MOFs is provided by the FT-IR spectra presented in Fig. 1(b). In Fe_3O_4/MOFs, the asymmetric stretching of the carboxylate groups in H_2BDC is detected at 1,508–1,623 cm^{-1}, and the symmetric stretching of carboxylate groups in H_2BDC is observed at 1,384 and 1,405 cm^{-1}. In the region of 1,300–600 cm^{-1}, several bands are observed, and they are assigned to the out-of-plane vibrations of H_2BDC. All the characteristic peaks indicate that Fe_3O_4/MOFs are successfully synthesized.

The texture of the composite Fe_3O_4/MOFs can be observed on SEM images presented in Fig. 2. It shows that the crystals of Fe_3O_4/MOFs are an aggregation of nanorods. The homogeneous structure stands for the formation of hybrid Fe_3O_4/MOFs, rather than simple mixture of Fe_3O_4 and MOFs.

Fig. 3 shows the N_2 adsorption–desorption isotherms and pore size distributions of Fe_3O_4/MOFs. It can be seen that both materials have certain adsorption capacity in the area of low pressure, and hysteresis loop in the area of medium and high pressure region. Curves show I/IV mixed-type isotherm, which means both materials are with microporous and mesoporous structures at the same time.

3.2. Adsorption

The removal effect for MB and MV in 5 min is shown in Fig. 4. It is clear that the color of dyes fade only in 5 min when Fe_3O_4/MOFs were added. It can be also seen that Fe_3O_4/MOFs gather in the vessel wall under magnetic force, which is obviously magnetic.

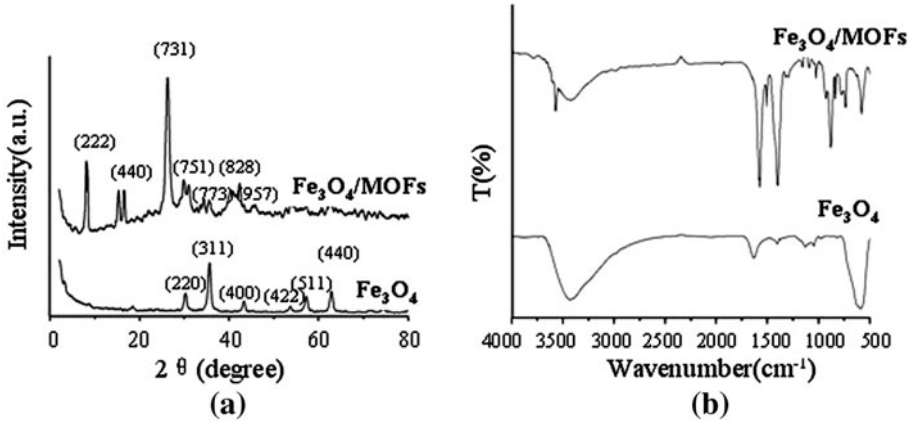

Fig. 1. XRD (a) and FT-IR spectra (b).

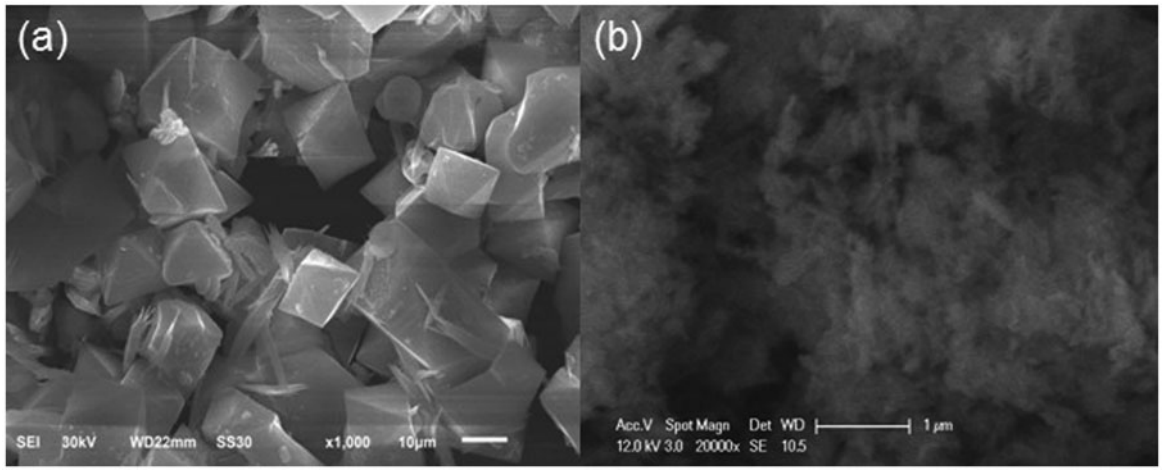

Fig. 2. SEM image for MOFs (a) and Fe_3O_4/MOFs (b).

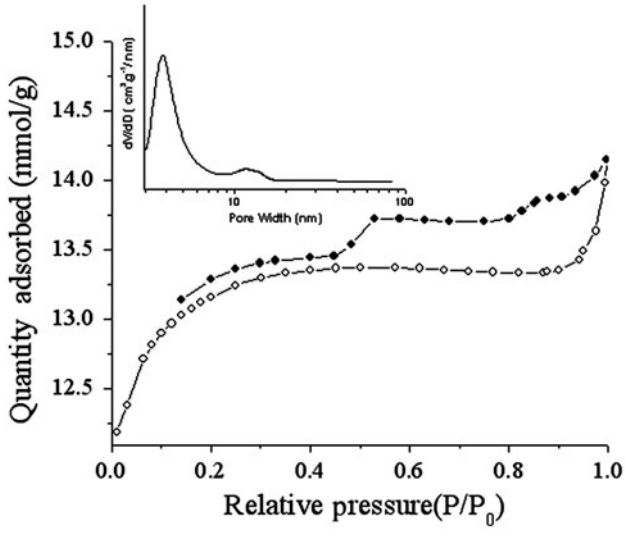

Fig. 3. N_2 adsorption–desorption isotherms and pore diameter distribution profiles (inset) of Fe_3O_4/MOFs.

The MB removal efficiency is shown in Fig. 5(a) and the MV removal efficiency is shown in Fig. 5(b). It shows that Fe_3O_4/MOFs have excellent removal efficiency. The removal efficiency of Fe_3O_4/MOFs can be high, above 90%, when the time is over 25 min.

3.3. Kinetics for the adsorption of MB and MV on Fe_3O_4/MOFs

The time-dependent adsorption capacity is obtained to study the kinetics for the adsorption of MB and MV on Fe_3O_4/MOFs. The adsorption model which describes the adsorption of a solute onto a solid surface can be expressed in the following way:

$$\frac{dq}{dt} = k_1(q_e - q_t) \tag{1}$$

where k_1 is the apparent pseudo-first-order constant (min^{-1}), q_t is the extent of adsorption at time t (in mg g^{-1}), and q_e is the extent of adsorption at equilibrium (mg g^{-1}). This law is used to describe processes in which the reaction rate, dq/dt, is proportional to the number of available sorption sites ($q_e - q_t$). The linear, integrated form of this equation for the boundary conditions; $q_t = 0$ at $t = 0$ and $q_t = q_t$ at $t = t$, can be written as:

$$\ln(q_e - q_t) = \ln q_e - k_1 t \tag{2}$$

Hence, the rate equation is obeyed when a linear relationship exists between log ($q_e - q_t$) and t, in which case k_1 may be estimated from the gradient of the plot. Similarly, the expression can be used to describe adsorption processes in which the reaction rate is proportional to the square of the number of available adsorption sites.

$$\frac{dq_t}{dt} = k_2(q_e - q_t)^2 \tag{3}$$

where k_2 is the apparent pseudo-second-order rate constant (in g mg^{-1} min^{-1}), and can be integrated and rearranged thus:

$$\frac{t}{q_t} = \frac{1}{k_2 q_e^2} + \frac{t}{q_e} \tag{4}$$

as a gradient of a linear plot of t/q_t against t.

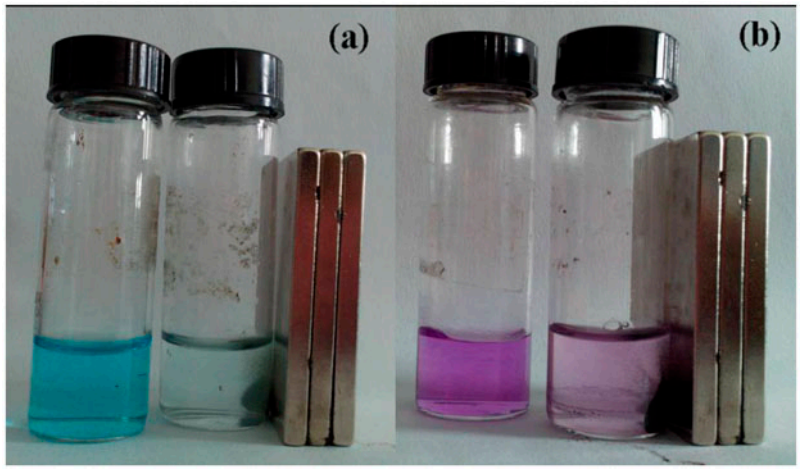

Fig. 4. MB removal (a) and MV removal (b) effect in 5 min.

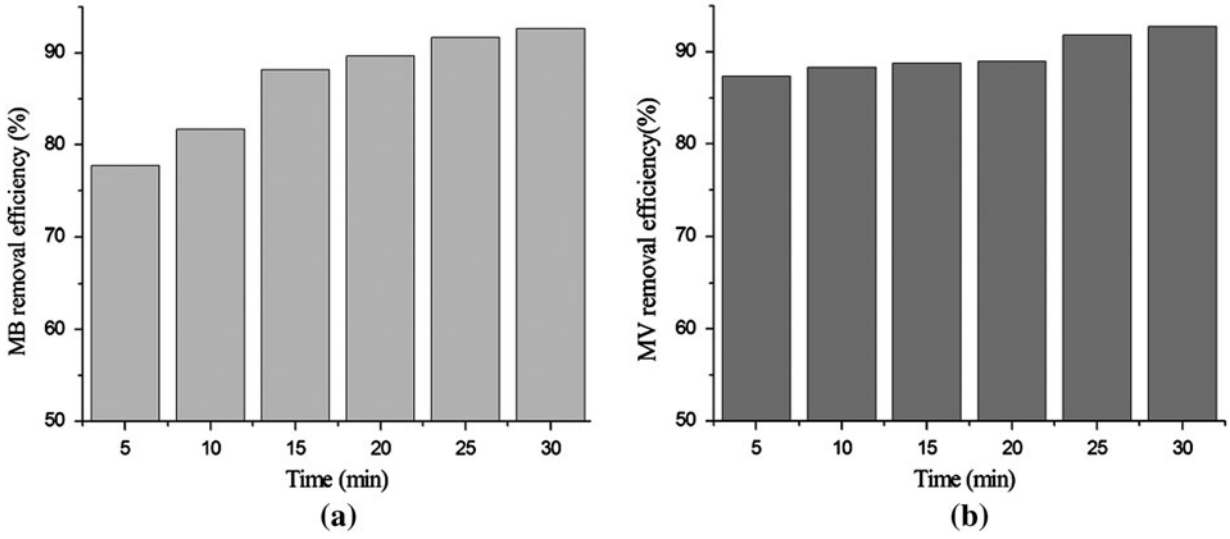

Fig. 5. Effect of time on the MB and MV elimination efficiencies.

The applicability of the pseudo-first- and pseudo-second-order kinetic models to the adsorption of MB and MV onto Fe_3O_4/MOFs have been tested by fitting the experimental data to the models by least-squares regression analysis, and it is found that pseudo-second-order kinetic model affords a more appropriate description of the adsorption process, as shown in Fig. 6.

3.4. Adsorption isotherms for MB and MV on Fe_3O_4/MOFs

To describe the adsorption isotherm more scientifically, the Freundlich model and Langmuir model are selected for this study. The Freundlich isotherm used for isothermal adsorption is a special case for heterogeneous surface energy in which the energy term in the Langmuir equation varies as a function of surface coverage strictly due to the variation of the sorption. The Freundlich equation is given as:

$$Qe = K_F Ce^{1/n} \tag{5}$$

where K_F and $1/n$ represents the Freundlich constants corresponding to adsorption capacity and adsorption intensity, respectively. A linear plot of ln Qe vs. ln Ce is obtained from the model as shown in Fig. 7. The correlation coefficient R^2 of the Freundlich equation for MV adsorption is 0.9918 and 0.9956 for MB adsorption.

The Langmuir adsorption isotherm has been successfully applied to many pollutant adsorption

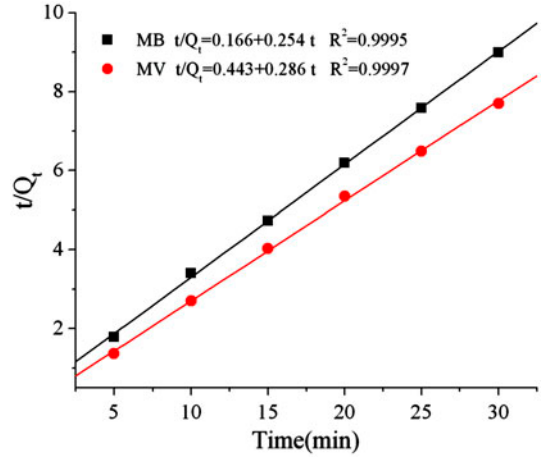

Fig. 6. Plots of pseudo-second-order kinetics for the adsorption of MB (a) and MV (b) on Fe_3O_4/MOFs.

processes from aqueous solution. The equation is expressed as:

$$Q_e = \frac{Q_0 K_L C_e}{1 + K_L C_e} \tag{6}$$

where Q_e: the equilibrium adsorption capacity of MB on the adsorbent (mg g^{-1}); C_e: the equilibrium MB concentration in solution (mg L^{-1}); Q_0: the maximum monolayer capacity of adsorbent (mg g^{-1}); and K_L: the Langmuir adsorption constant (L mg^{-1}), related to the free energy of adsorption. A linear plot of (C_e/Q_e) vs. C_e is obtained from the model as shown in Fig. 8. The correlation coefficient R^2 of the Langmuir equation for MV adsorption is 0.9991 and 0.9999 for MB adsorption. It shows that adsorption fits Langmuir model better, both for MB and MV.

3.5. Effect of recycled Fe_3O_4/MOFs on MB and MV adsorptions

To evaluate the possibility of regeneration and reusability of Fe_3O_4/MOFs as an adsorbent, desorption experiments are performed. Desorption and regeneration are achieved using methanol, ethanol, glycol, acetonitrile and acetone. The desorption efficiency of acetonitrile is the highest. The effect of five consecutive adsorption–desorption cycles is studied, and the results are shown in Fig. 9. It shows that the MB removal efficiency is still nearly 90% after five times recycle, and the MV removal efficiency is still above 95% after five times recycle. These results show that Fe_3O_4/MOFs are suitable for adsorbent and it can be recycled for dye adsorption.

Fe_3O_4/MOFs are applied in MSPE to determine the trace amount of MB and MV followed by UV–vis spectrophotometer. The results are shown in Table 1. The enrichment multiple for MB is 26, and the determination limit is 2.1 ng mL^{-1}. The enrichment multiple for MV is 65, and the determination limit is 6.0 ng mL^{-1}.

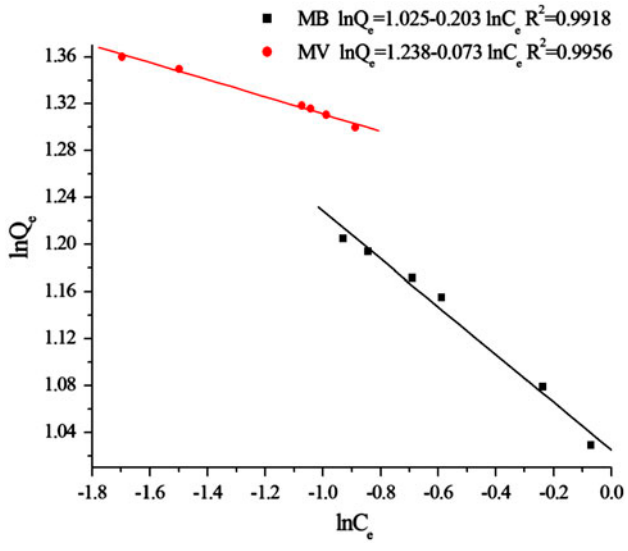

Fig. 7. Freundlich plots of the isotherms for MB adsorption (a) and MV adsorption (b) onto Fe_3O_4/MOFs.

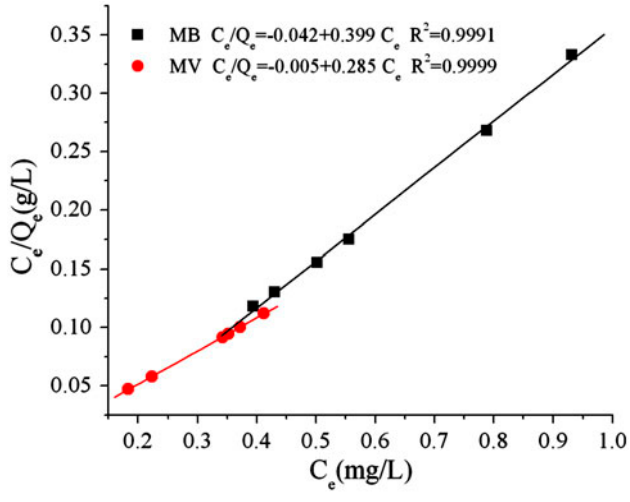

Fig. 8. Langmuir plots of the isotherms for MB adsorption (a) and MV adsorption (b) onto Fe_3O_4/MOFs.

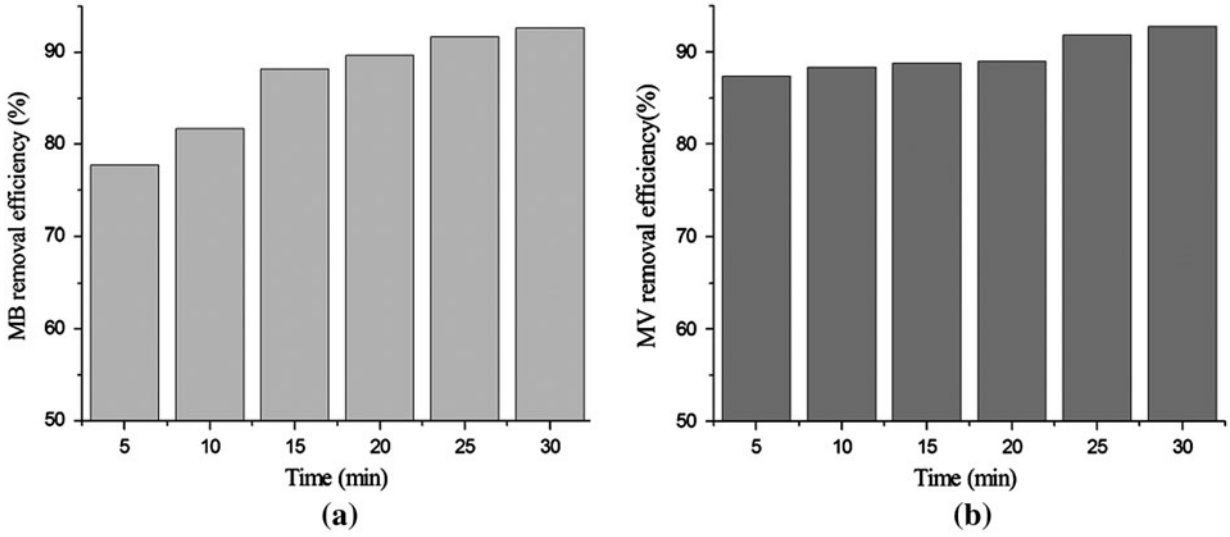

Fig. 9. (a) MB and (b) MV removal of recycled Fe_3O_4/MOFs.

Table 1
Sample analysis by SBSE-UV technique

Samples	Concentration ($\mu g\ L^{-1}$)	Preconcentration factors	Detection limit ($ng\ mL^{-1}$)
MB	96	90	1.5
MV	120	21	6.5

3.6. Analytical performance

The analytical performance of the procedure for MV and MB can be calculated from the results of spectrophotometric measurements. In order to estimate the accuracy of the procedure, different amounts of dyes are spiked in water and the resulting solutions are submitted to the preconcentration procedure. The results are given in Table 2. A good agreement can be obtained between the added and measured dyes. The recovery values for dyes are in the range of 95–105%. These values are quantitative and the presented method can be applied for the preconcentration of MV and MB in real samples.

Table 2
Tests of addition/recovery in the experiments for dyes, $N = 5$

Sample	Amount of dyes (μg)			Recovery (%)
	Added		Found	
Tap water	–		ND	
	MV	12.0	11.4	95.0
	MB	9.6	9.4	97.9
Tap water	–		ND	
	MV	24.0	25.0	104.2
	MB	19.2	18.6	96.9
Lake water	–		ND	
	MV	12.0	12.5	104.2
	MB	9.6	9.3	96.9

Note: ND: Not found.

4. Conclusions

In this work, Fe_3O_4/MOFs are introduced for the adsorptive removal of MB and MV from wastewater. The results indicate that pseudo-second-order kinetic model matched with the adsorption of MB and MV onto Fe_3O_4/MOFs. The Langmuir model fits the data of the adsorption. Fe_3O_4/MOFs can be recycled to use at least five times, therefore, Fe_3O_4/MOFs have a great prospect in the dye adsorption area in dyeing wastewater treatment. Furthermore, Fe_3O_4/MOFs can be successfully applied in MSPE to determine the trace amount of MB and MV followed by UV–vis spectrophotometer.

Acknowledgments

Project supported by the National Natural Science Foundation of China (Grant No. 51302071).

References

[1] G. Crini, Non-conventional low-cost adsorbents for dye removal: A review, Bioresour. Technol. 97 (2006) 1061–1085.

[2] Y.S. Al-Degs, M.I. El-Barghouthi, M.A. Khraisheh, M.N. Ahmad, S.J. Allen, Effect of surface area, micropores, secondary micropores, and mesopores volumes of activated carbons on reactive dyes from solution, Sep. Sci. Technol. 39 (2004) 97–111.
[3] S.H. Chen, J. Zhang, C.L. Zhang, Q.Y. Yue, Y. Li, C. Li, Equilibrium and kinetic studies of methyl orange and methyl violet adsorption on activated carbon derived from *Phragmites australis*, Desalination 252 (2010) 149–156.
[4] E.I. Unuabonah, K.O. Adebowale, F.A. Dawodu, Equilibrium, kinetic and sorber design studies on the adsorption of Aniline blue dye by sodium tetraborate-modified Kaolinite clay adsorbent, J. Hazard. Mater. 157 (2008) 397–409.
[5] L.G. da Silva, R. Ruggiero, P.D. Gontijo, R.B. Pinto, B. Royer, E.C. Lima, T. Fernandes, T. Calvete, Adsorption of Brilliant Red 2BE dye from water solutions by a chemically modified sugarcane bagasse lignin, Chem. Eng. J. 168 (2011) 620–628.
[6] U. Müller, M.M. Schubert, O.M. Yaghi, Characterization of Solid Catalysts, in: U. Müller, M.M. Schubert, O.M. Yaghi (Eds.), Handbook of Heterogeneous Catalysis Wiley-VCH Verlag GmbH & Co. KGaA, Weinheim, 2008, 247–262.
[7] A. Bagheri, M. Taghizadeh, M. Behbahani, A.A. Akbar Asgharinezhad, M. Salarian, A. Dehghani, H. Ebrahimzadeh, M.M. Amini, Synthesis and characterization of magnetic metal-organic framework (MOF) as a novel sorbent, and its optimization by experimental design methodology for determination of palladium in environmental samples, Talanta 99 (2012) 132–139.
[8] C. Petit, T.J. Bandosz, Exploring the coordination chemistry of MOF–graphite oxide composites and their applications as adsorbents, Dalton Trans. 41 (2012) 4027–4035.
[9] C. Chen, M. Zhang, Q.X. Guan, W. Li, Kinetic and thermodynamic studies on the adsorption of xylenol orange onto MIL-101(Cr), Chem. Eng. J. 183 (2012) 60–67.
[10] L. Li, F.X. Sun, J.T. Jia, T. Borjigin, G.S. Zhu, Growth of large single MOF crystals and effective separation of organic dyes, Cryst. Eng. Comm. 15 (2013) 4094–4098.
[11] X.X. Huang, L.G. Qiu, W. Zhang, Y.P. Yuan, X. Jiang, A.J. Xie, Y.H. Shen, J.F. Zhu, Hierarchically mesostructured MIL-101 metal–organic frameworks: Supramolecular template-directed synthesis and accelerated adsorption kinetics for dye removal, Cryst. Eng. Comm. 14 (2012) 1613–1617.
[12] M. Carboni, C.W. Abney, S.B. Liu, W.B. Lin, Highly porous and stable metal–organic frameworks for uranium extraction, Chem. Sci. 4 (2013) 2396–2402.
[13] W.L. Liu, S.H. Lo, B. Singco, C.C. Yang, H.Y. Huang, C.H. Lin, Novel trypsin–FITC@MOF bioreactor efficiently catalyzes protein digestion, J. Mater. Chem. B 1 (2013) 928–932.
[14] T.J. Bandosz, C. Petit, MOF/graphite oxide hybrid materials: Exploring the new concept of adsorbents and catalysts, Adsorption 17 (2011) 5–16.
[15] S.L. Zhang, Z. Du, G.K. Li, Metal-organic framework-199/graphite oxide hybrid composites coated solid-phase microextraction fibers coupled with gas chromatography for determination of organochlorine pesticides from complicated samples, Talanta 115 (2013) 32–39.
[16] H.L. Jiang, Q. Xu, Porous metal–organic frameworks as platforms for functional applications, Chem. Commun. 47 (2011) 3351–3370.
[17] Q. Han, Z.H. Wang, J.F. Xia, Facile and tunable fabrication of Fe_3O_4/graphene oxide nanocomposites and their application in the magnetic solid-phase extraction of polycyclic aromatic hydrocarbons from environmental water samples, Talanta 101 (2012) 388–395.
[18] F. Ke, Y.P. Yuan, L.G. Qiu, Y.H. Shen, A.J. Xie, J.F. Zhu, X.Y. Tian, L.D. Zhang, Facile fabrication of magnetic metal–organic framework nanocomposites for potential targeted drug delivery, J. Mater. Chem. 21 (2011) 3843–3848.
[19] M. Mikhaylova, D.K. Kim, N. Bobrysheva, M. Osmolowsky, V. Semenov, T. Tsakalakos, M. Muhammed, Superparamagnetism of magnetite nanoparticles: Dependence on surface modification, Langmuir 20 (2004) 2472–2477.